

Beyond-the-Standard Model Higgs Physics using the ATLAS Experiment

Loan Truong^{1,2,3a} on behalf of the ATLAS Collaboration

¹*INFN Gruppo Collegato di Udine, Sezione di Trieste, Udine, Italy*

²*ICTP, Trieste, Italy*

³*SISSA, Trieste, Italy*

Abstract. Recent searches for the Higgs boson in the context of beyond the Standard Model performed by the ATLAS experiment are presented: high mass Higgs boson searches, lepton flavour violating Higgs decay, NMSSM, constraint from the search for three photons. The interpretation based on the measurements of Higgs couplings is shown, along with the constraint on the Higgs boson invisible decays. The search for invisible decays of a Higgs boson produced in association with a Z boson was performed with both $\sqrt{s} = 7$ and 8 TeV while the rest were performed using the $\sqrt{s} = 8$ TeV data of proton-proton collisions collected by the ATLAS experiment. No significant excess of data over the predicted background is observed and limits are placed in certain quantities depending on the searches.

1 Introduction

The ATLAS experiment at the LHC discovered the Higgs boson in July 2012. So far, there have been many measurements on its couplings and mass [1–5], the results are consistent with the Standard Model (SM) predictions. Nevertheless, these measurements have not yet excluded a large range of other extensions of the SM.

Exploring whether there are additional Higgs bosons or exotic decay of the SM Higgs boson can give us direct evidences about physics beyond the Standard Model (BSM). Those include the two Higgs doublet models (2HDMs) [6–9], next-to-minimal supersymmetric SM (NMSSM) [10, 11], composite Higgs models [12, 13], which favour the existence of other Higgs bosons in the high-mass regime, as well as lepton flavour violating (LFV) Higgs decay, three photons Higgs decay. There are strong evidences of dark matter from astrophysical observations which could be explained by the existence of weakly interacting massive particles (WIMPs, see Ref. [14] and the references therein). The observed Higgs boson might decay to dark matter or other stable or long-lived particles which do not interact significantly with a detector [15–19] leading to Higgs boson invisible decay.

The report is organized as follows: Sec. 2 describes the high mass-Higgs boson searches, Sec. 3 describes the LFV Higgs decay search, Sec. 4 describes the search for Higgs bosons

^ae-mail: lotruong@cern.ch

in the context of NMSSM, Sec. 5 describes the search for a Higgs boson decaying to three photons or more, Sec. 6 summarizes some constraints on BSM models using Higgs boson couplings and mass measurements, Sec. 7 describes the combination of the searches for invisible decays of the Higgs boson. Finally concluding remarks are in Sec. 8. Details about the ATLAS detector can be found in Ref. [20].

2 High masses searches

Two searches for a high-mass Higgs boson H were performed in the $H \rightarrow WW \rightarrow \ell\nu\ell\nu, \ell\nu qq$ [21] and $H \rightarrow ZZ \rightarrow \ell\ell\ell\ell, \ell\ell\nu\nu, \ell\ell qq, \nu\nu qq$ [22] channels. No significant deviations were observed. The results were interpreted separately for VBF, ggF production modes as upper limits at 95% CL (see Fig. 1 and Tab. 1) on $\sigma_H \times BR(H \rightarrow WW/ZZ)$ for heavy Higgs boson which has a narrow width.

Table 1: Upper limits on the production cross section of the high mass-Higgs boson in different weak vector boson decay modes [21, 22].

Limits on	m_H [GeV]	Upper Limit [fb] for H production mode	
		ggF	VBF
$\sigma_H \times BR(H \rightarrow WW)$	1500	21	6
$\sigma_H \times BR(H \rightarrow ZZ)$	195 ÷ 950	530 ÷ 8	310 ÷ 9

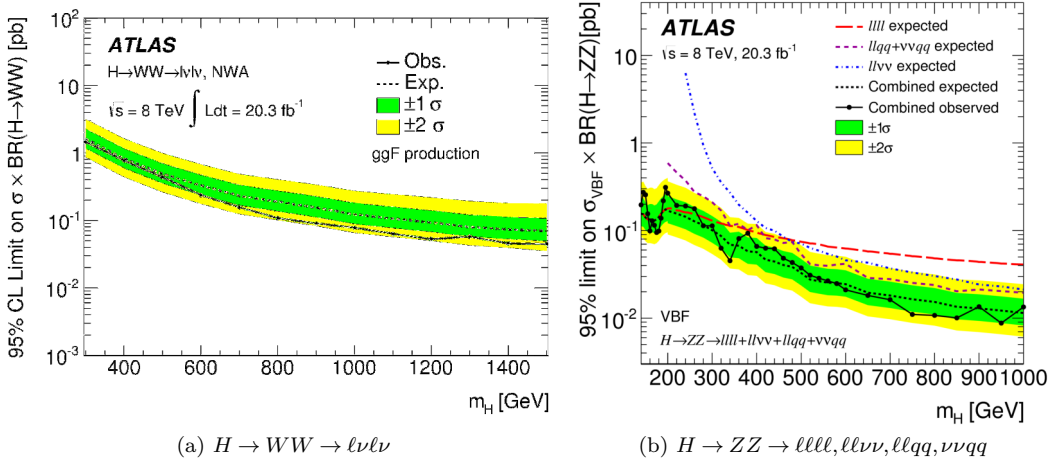


Figure 1: Limits set on the production cross section of the high mass-Higgs boson in (a) WW [21], (b) ZZ [22] resonance searches.

3 Lepton flavour violating decays

The LFV Higgs decays ($H \rightarrow \tau\mu, \tau e, \mu e$) arise at tree level based on assumed flavour violating Yukawa interactions [23]. A search for LFV Higgs decays was done in the channel $H \rightarrow \mu\tau_{had}$

in hadronic τ decays [24]. A fit to the reconstructed mass distribution in data was performed (see Fig. 2) resulting in the best fit of $BR(H \rightarrow \mu\tau) = 0.77 \pm 0.62\%$, upper limit on $BR(H \rightarrow \mu\tau)$ at 95% CL: 1.85%(1.24%) obs(exp).

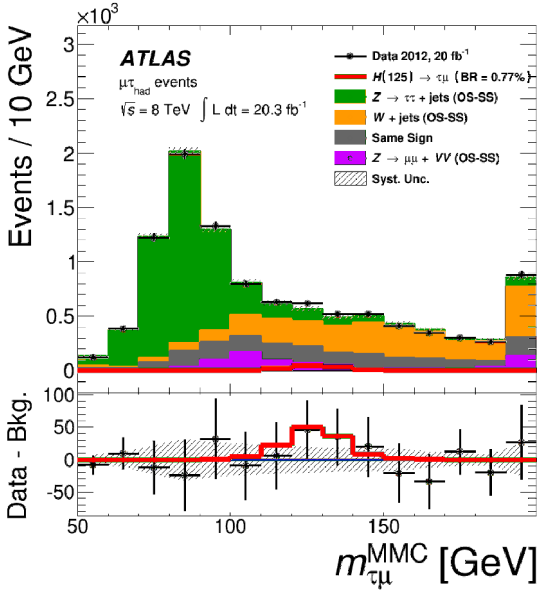


Figure 2. The reconstructed mass of the system of observed muon, τ (hadronic decay products) & E_T^{miss} objects [24] by means of the Missing Mass Calculator distribution.

4 NMSSM

The NMSSM contains an additional pseudoscalar Higgs boson (a), generally assumed to have a mass lower than the observed Higgs boson (h) since its mass is protected by a Peccei–Quinn symmetry. A search for the decay to a pair of the lightest neutral pseudoscalar Higgs a of either the 125 GeV Higgs (h) or a second CP-even Higgs (H) was performed [25], where one a boson decays to 2μ and the other decays to 2τ . As a result, the most stringent upper limit on the branching ratio of the h boson decaying to the non-SM particles was set at 3.5% for $m_a = 3.75$ GeV (see Fig. 3).

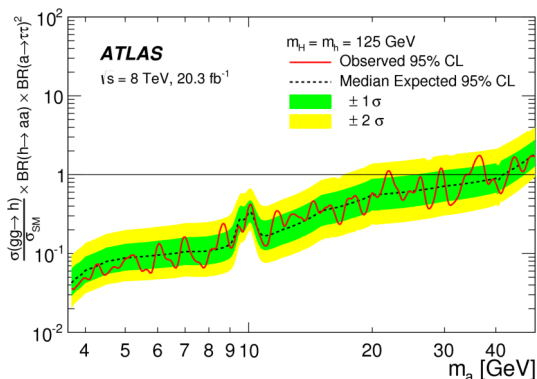


Figure 3. Limit for $\sigma_{gg} H_{SM} \times BR$ of h SM decays to $aa \times BR$ of a decays to $\tau\tau$ vs m_a [25].

5 Search for 3 photons

A search for events with at least 3 γ was done [26]. The model-independent interpretations are the first of their kind. One of the interpretations was performed for a SM Higgs boson (h) decaying to four photons via a pair of intermediate pseudoscalar particles (a). Limits on the cross section times $BR(h \rightarrow aa) \times BR(a \rightarrow \gamma\gamma)^2$ was set to be $< 10^{-3} \sigma_{SM}$ for $10 \text{ GeV} < m_a < 62 \text{ GeV}$ (see Fig. 4).

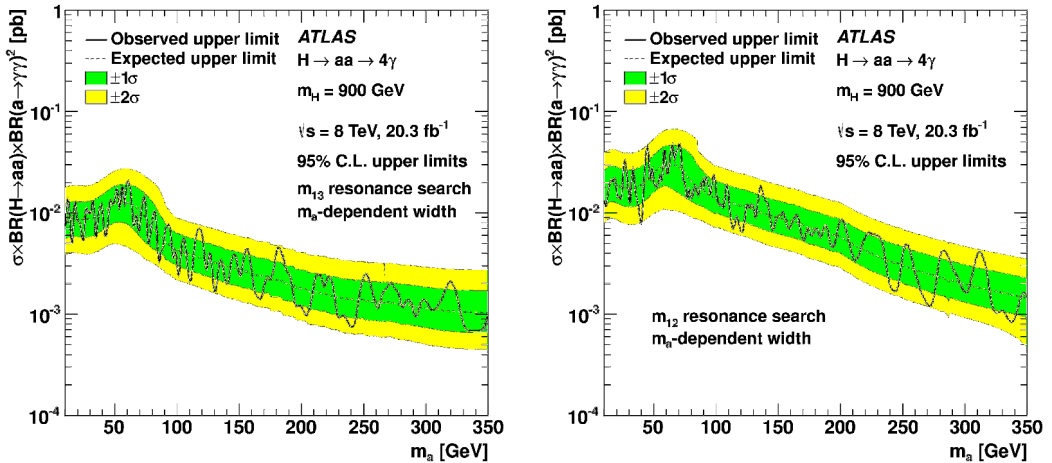


Figure 4: Left: For SM Higgs $h \rightarrow aa \rightarrow \gamma\gamma\gamma\gamma$: $\sigma \times BR(h \rightarrow aa) \times BR(a \rightarrow \gamma\gamma)^2 < 10^{-3} \times \sigma_{SM}$ for $10 \text{ GeV} < m_a < 62 \text{ GeV}$. Right: for heavy Higgs boson-like scalar: $\sigma_H \times BR(H \rightarrow aa) \times BR(a \rightarrow \gamma\gamma)^2 < 0.02$ to 0.001 pb (depending upon m_H, m_a) [26].

6 Beyond the Standard Model constraints via Higgs boson couplings

BSM constraints [27] were performed using the measured production and decay rates of the Higgs boson ($\gamma\gamma$, ZZ , WW , $Z\gamma$, $b\bar{b}$, $\tau\tau$, & $\mu\mu$; $t\bar{t}h$ with $h \rightarrow \gamma\gamma$, $b\bar{b}$ & multileptons). The constraints include the probe on the scaling of the couplings with mass, setting limits on parameters in extensions of the SM such as composite Higgs boson, 2HDMs. They are described in details below.

6.1 Mass scaling of couplings

In this analysis, the observed rates in different channels were used in a fit to determine how the Higgs boson couplings to other particles scale with the masses of those particles [28]. Each coupling (with fermion f and boson V) was scaled in terms of “vacuum expectation value (vev)” M and mass scaling parameter ϵ (in the SM $\text{vev } v \approx 246 \text{ GeV}$ and $\epsilon \rightarrow 0$) as $\kappa_f = v \frac{m_f^\epsilon}{M^{1+\epsilon}}$, $\kappa_V = v \frac{m_V^{2\epsilon}}{M^{1+2\epsilon}}$, where m is the mass of the particle. As a result of the fit, the best fit value is consistent within one standard deviation with the SM (see Fig. 5), observed values for ϵ and M are shown in Tab. 2.

Table 2: Observed and expected measurements of the mass scaling parameter ϵ and the vev parameter M [27].

Parameter	Obs.	Exp.
ϵ	0.018 ± 0.039	0.000 ± 0.042
M	224^{+14}_{-12} GeV	246^{+19}_{-16} GeV

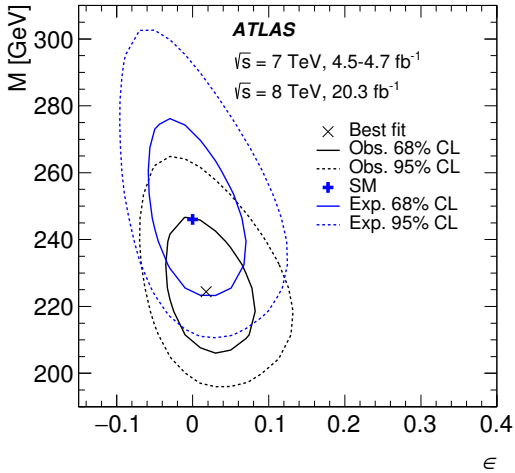


Figure 5. 2-D confidence intervals as a function of the mass scaling factor ϵ and the vev parameter M [27].

6.2 Minimal composite Higgs model

Minimal Composite Higgs Models (MCHM) [12, 13] provides a possible explanation for the scalar naturalness problem. It suggests that the Higgs boson is a composite, pseudo-Nambu–Goldstone boson rather than an elementary particle. Higgs couplings are modified as functions of compositeness scale- f : $\xi = v^2/f^2$. There are different MCHM models with different modifications of the Higgs coupling such as MCHM4 [12] with $\sqrt{\kappa} = \kappa_V = \kappa_F = 1 - \xi$ and MCHM5 [13] with $\kappa_V = 1 - \xi, \kappa_F = \frac{1-2\xi}{\sqrt{1-\xi}}$. The SM is recovered in the limit $\xi \rightarrow 0$, namely $f \rightarrow \infty$. A fit was performed in the parameter space of $[\kappa_F, \kappa_V]$ (see Fig. 6). As a result, limits at 95% CL are obtained in the order of obs (exp), for MCHM4: $f > 710$ (510) GeV, MCHM5: $f > 780$ (600) GeV.

6.3 Two Higgs Doublet Models

2HDMs models introduce two complex SU(2) doublets of scalar fields and there are 4 types of them (as summarized in Tab. 3). They predict five Higgs bosons: two neutral CP-even bosons h and H , one neutral CP-odd boson A , and two charged bosons H^\pm . When considering the CP-conserving case, there are 6 sensitive parameters in the analysis: 4 masses m_h, m_H, m_{H^\pm}, m_A & 2 mixing angles α, β . Where $\tan\beta = v_1/v_2$ is the ratio of the two Higgs doublets' vevs which satisfy $v_1^2 + v_2^2 = v^2 \approx (246 \text{ GeV})^2$, α : mixing angle between h & H . Assumptions for interpretations are that the 125 GeV boson is the light Higgs, no radiative corrections from BSM for the production of Higgs boson, only SM decays. Gauge invariance requires the

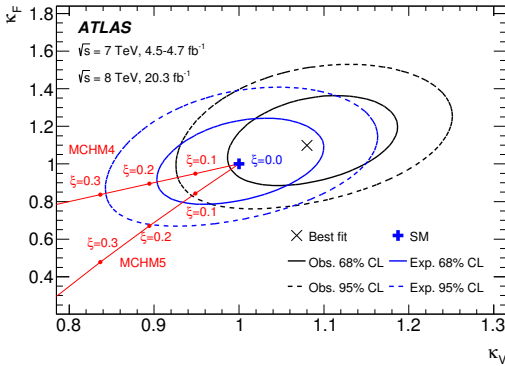


Figure 6. 2-D likelihood contours in the (κ_V, κ_F) coupling scale factor plane [27].

Table 3: Couplings of the light Higgs boson h to weak vector bosons (κ_V), up-type quarks (κ_u), down-type quarks (κ_d), and charged leptons (κ_ℓ), expressed as ratios to the corresponding SM predictions in 2HDMs of various types.

Coupling scale factor	Type I (fermiophobic)	Type II (MSSM-like)	Lepton-specific	Flipped
κ_V		$\sin(\beta - \alpha)$		
κ_u		$\cos(\alpha) / \sin(\beta)$		
κ_d	$\cos(\alpha) / \sin(\beta)$	$-\sin(\alpha) / \cos(\beta)$	$\cos(\alpha) / \sin(\beta)$	$-\sin(\alpha) / \cos(\beta)$
κ_ℓ	$\cos(\alpha) / \sin(\beta)$	$-\sin(\alpha) / \cos(\beta)$	$-\sin(\alpha) / \cos(\beta)$	$\cos(\alpha) / \sin(\beta)$

couplings of the two neutral, CP-even Higgs bosons to vector bosons relative to their SM values to be:

$$\begin{aligned} g_{hVV}^{2HDM} / g_{hVV}^{SM} &= \sin(\beta - \alpha) \\ g_{HVV}^{2HDM} / g_{HVV}^{SM} &= \cos(\beta - \alpha) \end{aligned} \quad (1)$$

with the convention: $\sin(\beta - \alpha) \geq 0$. SM-like alignment limit is retrieved at $\cos(\beta - \alpha) = 0$.

Figure 7 shows the regions of the $[\cos(\beta - \alpha), \tan \beta]$ plane that are excluded at 95% CL for each of the four types of 2HDMs, overlaid with the exclusion limits expected for the SM Higgs sector. A physical boundary of $\kappa_V \leq 1$ is there in all four 2HDM types and restricts the profile likelihood ratio. The data are consistent with the alignment limit within approximately one standard deviation or better in each of the model.

7 Higgs invisible decays

Limits on the branching ratio of Higgs boson invisible decay [27] are set and subsequently used to constrain on a Higgs-portal dark matter model [29].

7.1 The combination of Higgs invisible decay channels

Direct searches for the SM Higgs boson h decaying into invisible particles used the following strategies: selecting events with large missing transverse momentum (E_T^{miss}), using particles

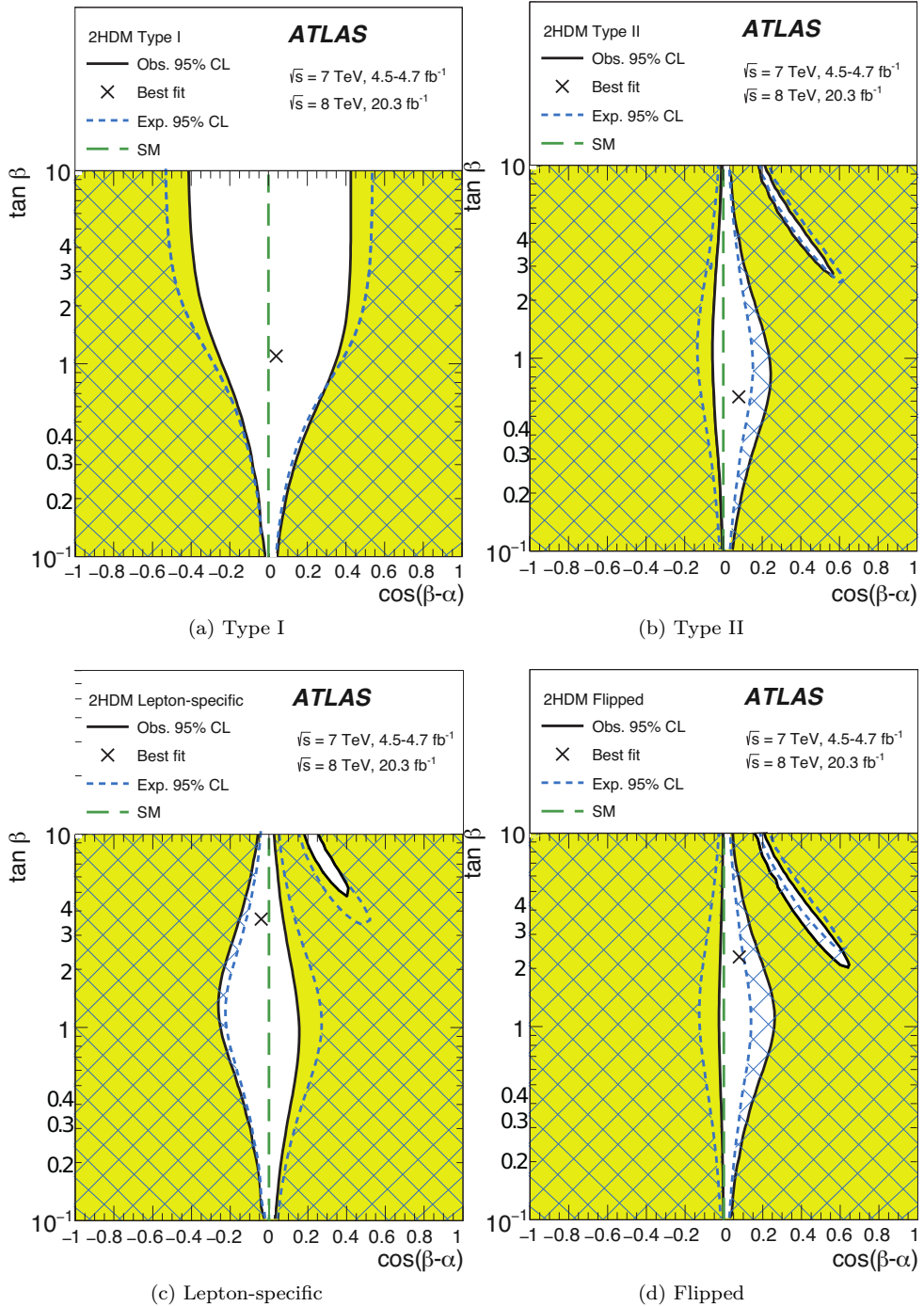


Figure 7: Regions of the $(\cos(\beta - \alpha), \tan \beta)$ plane of four types of 2HDMs excluded by fits to the measured rates of Higgs boson production and decays. The likelihood contours where $-2 \ln \Lambda = 6.0$, corresponding approximately to the 95% CL (2 std. dev.), are indicated for both the data and the expectation assuming the SM Higgs sector. The cross in each plot marks the observed best-fit value. The light shaded and hashed regions indicate the observed and expected exclusions, respectively. The plots are shown for $\sin(\beta - \alpha) \geq 0$ without loss of generality [27].

produced associated with the Higgs boson to tag the Higgs, assuming productions (and acceptance) as in the SM where $BR(h \rightarrow ZZ \rightarrow 4\nu) = 1.2 \times 10^{-3}$. The SM branching ratio is very little so any observation would be an indication of BSM physics. They include the analyses: $Z(\rightarrow \ell\ell) h \rightarrow inv$ (E_T^{miss}) [30], $W/Z(\rightarrow jj) h \rightarrow inv$ (E_T^{miss}) [31], VBF ($\rightarrow jj$) $h \rightarrow inv$ (E_T^{miss}) [32], where the first analysis contains the 7 TeV data.

Table 4 shows upper limits on the $BR(h \rightarrow inv)$ at 95% CL and other CL for different analyses and their statistical combination. The combination of the invisible channels only resulted in $BR(h \rightarrow inv) < 0.25$ obs (0.27 exp).

Table 4: Summary of upper bounds on $BR(h \rightarrow inv)$ [27].

Results	Observed	-2σ	-1σ	Expected	$+1\sigma$	$+2\sigma$
VBF h	0.28	0.16	0.21	0.31	0.41	0.56
$Z(\rightarrow \ell\ell)h$	0.75	0.33	0.45	0.62	0.86	1.19
$V(\rightarrow jj)h$	0.78	0.46	0.62	0.86	1.19	1.60
Combined Results	0.25	0.13	0.18	0.27	0.35	0.47

Combined result was then combined statistically with the measured visible decay rates of the Higgs boson. A physical boundary of $BR_{inv} > 0$ was required. The most general result uses independent coupling parameters $\kappa_W, \kappa_Z, \kappa_t, \kappa_b, \kappa_\tau, \kappa_\mu, \kappa_g, \kappa_\gamma, \kappa_{Z\gamma}$ and BR_{inv} . Upper limit of 0.23(0.24) obs(exp.) were set at 95% CL. The likelihood scan for that statistical fit is shown in Fig. 8.

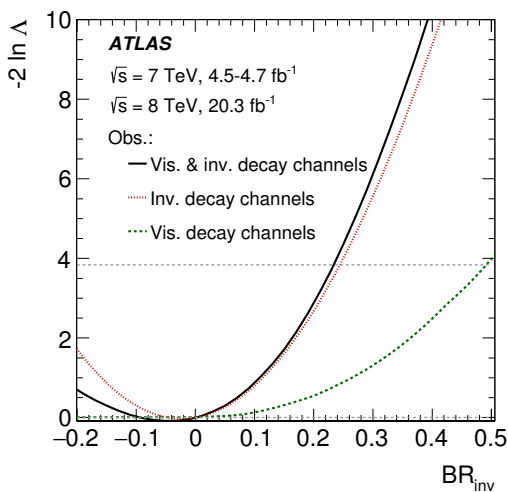


Figure 8. Likelihood scans of the Higgs' invisible branching ratio [27].

7.2 Higgs Portal Interpretation

The 90%CL upper limit of 0.22 (0.23) obs (exp) on $BR(H \rightarrow inv)$ was used to constrain on a Higgs-portal dark matter scenario [29], where the Higgs boson is the only mediator for interactions between WIMPs and other SM particles. It is sensitive for WIMP's mass $< m_h/2$. Limits are set on the cross section between WIMPs and nucleons as a function of the

- [11] D. Curtin et al., Phys. Rev. **D90**, 075004 (2014), 1312.4992
- [12] K. Agashe, R. Contino, A. Pomarol, Nucl. Phys. **B 719**, 165 (2005), hep-ph/0412089
- [13] R. Contino, L. Da Rold, A. Pomarol, Phys. Rev. D **75**, 055014 (2007)
- [14] D.C. et al., Astrophys. J. **648**, L109 (2006), astro-ph/0608407
- [15] I. Antoniadis, M. Tuckmantel, F. Zwirner, Nucl.Phys. **B707**, 215 (2005), hep-ph/0410165
- [16] N. Arkani-Hamed, S. Dimopoulos, G. Dvali, J. March-Russell, Phys.Rev. **D65**, 024032 (2002), hep-ph/9811448
- [17] A. Datta, K. Huitu, J. Laamanen, B. Mukhopadhyaya, Phys.Rev. **D70**, 075003 (2004), hep-ph/0404056
- [18] S. Kanemura, S. Matsumoto, T. Nabeshima, N. Okada, Phys.Rev. **D82**, 055026 (2010), 1005.5651
- [19] A. Djouadi, A. Falkowski, Y. Mambrini, J. Quevillon, Eur.Phys.J. **C73**, 2455 (2013), 1205.3169
- [20] ATLAS Collaboration, JINST **3**, S08003 (2008)
- [21] ATLAS Collaboration (2015), 1509.00389
- [22] ATLAS Collaboration (2015), 1507.05930
- [23] R. Harnik, J. Kopp, J. Zupan, JHEP **03**, 026 (2013), 1209.1397
- [24] ATLAS Collaboration (2015), 1508.03372
- [25] ATLAS Collaboration, Phys. Rev. **D92**, 052002 (2015), 1505.01609
- [26] ATLAS Collaboration (2015), 1509.05051
- [27] ATLAS Collaboration (2015), 1509.00672
- [28] J. Ellis, T. You, JHEP **06**, 103 (2013), 1303.3879
- [29] A. Djouadi, O. Lebedev, Y. Mambrini, J. Quevillon, Phys.Lett. **B709**, 65 (2012), 1112.3299
- [30] ATLAS Collaboration (ATLAS), Phys. Rev. Lett. **112**, 201802 (2014), 1402.3244
- [31] ATLAS Collaboration (ATLAS), Eur. Phys. J. **C75**, 337 (2015), 1504.04324
- [32] ATLAS Collaboration (2015), 1508.07869